Shock propagation in a granular chain

Erwan Hascoët,[1] Hans J. Herrmann,[1,2] and Vittorio Loreto[1]
[1]*PMMH Ecole Supérieure de Physique et Chimie Industrielles, 10 rue Vauquelin, 75231 Paris Cedex 05, France*
[2]*ICA1, University of Stuttgart, Pfaffenwaldring 27, D-70569 Stuttgart, Germany*
(Received 22 January 1998; revised manuscript received 14 September 1998)

We numerically solve the propagation of a shock wave in a chain of elastic beads with no restoring forces under traction (no-tension elasticity). We find a sequence of peaks of decreasing amplitude and velocity. Analyzing the main peak at different times we confirm a recently proposed scaling law for its decay. [S1063-651X(99)07903-9]

PACS number(s): 81.05.Rm

I. INTRODUCTION

The study of granular matter is of interest for fundamental physics as well as for technological applications. The intensive studies of liquids and solids gave physicists powerful tools for investigating these states of matter. These tools are, however, very difficult to apply to granular matter [1].

Little work has been done on sound propagation in real granular media. Experiments have been performed by Liu and Nagel [2–4] who investigated the propagation of low amplitude vibrations in a box of spherical beads. It was concluded that nonlinearity and disorder make wave propagation behave in very unexpected ways: the fragile structure of contacts between grains makes them sensitive to rearrangements, dramatically changing the amplitude response of the receptor to the source. Besides, disorder gives rise to important interference effects that can lead to localization [5]. Numerical simulations have been made by Melin [6], who studied the depth dependence of sound speed in granular media. The results obtained were different from the power law behavior between sound speed and pressure predicted by Goddard [7] in an effective medium calculation.

Three-dimensional models seem to be very difficult to investigate directly and we need to begin with simplified models in order to isolate specific features of real granular media. In this paper we try to understand the effect of nonlinearity on wave propagation in one dimension. A previous study was done by Nesterenko [8] on a chain of spherical beads obeying the elastic Hertz law of contact. It was shown both analytically and numerically that the chain submitted to compression pulses involves solitary wave propagation. This has been confirmed by the experiments of Lazaridi and Nesterenko [9] and of Coste, Falcon, and Fauve [10].

Here, we want to study the case of a chain of beads initially in contact and submitted to a shock perturbation. The beads interact via an elastic contact law only when they are compressed. The problem is therefore highly nonlinear because as soon as there are broken contacts the chain behaves as an ensemble of independent elastic systems. We can look at this problem even in terms of a linear chain of points connected by springs with completely asymmetric elastic constants: k in compression and zero in extension. Here we must emphasize that the Hertz law which has been studied until now corresponds to perfect spherical beads. In a real granular medium the shape of the beads at contacts can be far from spherical. In fact bead interactions can be modeled with a force law exponent varying from 1 to 2. Our linear compression force model belongs to this range. This one-dimensional system is clearly far from being realistic but it exhibits some features which can aid understanding of the more general problem. In particular, we try to elucidate how the front wave propagates and how its lost energy can contribute to the formation of several other secondary waves. The outline of the paper is as follows. In Sec. II we define our model and we present the setup for the numerical simulations. Section III is devoted to the description of the results concerning the phenomenology of the system. In Sec. IV we discuss in detail the mechanism of front formation. Discussions and conclusion will be given in Sec. V.

II. MODEL DEFINITION

Our model is composed of N spherical beads of radius R and mass m. We define the force between two neighboring beads as varying linearly under compression and being equal to zero when the beads are not in contact. It can be written as

$$F = k\,\delta\,\theta(\delta), \tag{1}$$

where k is the spring constant, $2R-\delta$ the distance between the centers of the two neighboring beads, and θ the Heaviside function. Mechanically such systems are known as ''no-tension elastic'' [12]. Initially all the beads are just touching each other without exerting any forces on each other except for the first bead which penetrates the second one by δ_0. We then let the system evolve with the left end fixed and the right end free. An experimental realization of the model can easily be done, as can be seen from Fig. 1. This one-dimensional array of nonconnected linear springs is the simplest model for no-tension elasticity. The equations of motion are the following:

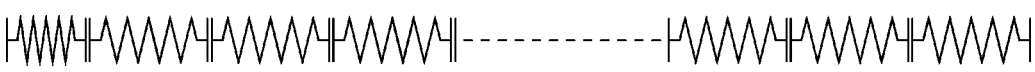

FIG. 1. Simple experimental realization of the model.

$$m\ddot{u}_i = k\delta_{i-1,i}\theta(\delta_{i-1,i}) - k\delta_{i,i+1}\theta(\delta_{i,i+1}), \quad 0<i<N-1 \tag{2}$$

where u_i is the displacement of bead number i. One can write

$$\delta_{i-1,i} = 2R - (x_i - x_{i-1}) \tag{3}$$

$$= 2R - [u_i + x_{i,0} - (u_{i-1} + x_{i-1,0})] \tag{4}$$

$$= u_{i-1} - u_i, \tag{5}$$

where x_i is the position of bead number i and $x_{i,0} = (2i+1)R$. Thus,

$$m\ddot{u}_i = k(u_{i-1} - u_i)\theta(u_{i-1} - u_i) - k(u_i - u_{i+1})\theta(u_i - u_{i+1}), \quad 0<i<N-1 \tag{6}$$

with the boundary conditions given by

$$u_0 = \delta_0 \quad \text{for } t \geq 0,$$

$$u_i = 0 \quad \text{for } i>0 \quad \text{and } t=0. \tag{7}$$

These boundary conditions correspond to the study of the propagation of a shock in the chain. From now on we will denote with forward and backward direction the direction of increasing and decreasing i, respectively. For the numerical implementation of the analysis we have chosen $N=1500$, $R=5$ mm, $\rho = 1.9\times 10^3$ kg m^{-3}, $k = 10^7$ N m^{-1}, and $\delta_0 = 0.5$ mm. Several algorithms have been used to solve the system of equations (6). First, we implemented the Verlet scheme which was not able to give good enough precision. Much better accuracy was obtained with a fifth order Gear predictor-corrector method being even more precise than the fourth order Runge-Kutta scheme. The test of the accuracy was obtained by monitoring the energy conservation of the system. During the computation, energy conservation was satisfied with a relative error lower than 10^{-6} with a time step $\Delta t = 10^{-8}$ s. It is worth stressing that during the total time of evolution the perturbation never reaches the end of the chain.

III. FRONT PHENOMENOLOGY AND COMPARISON WITH THE HARMONIC CASE

In order to follow the evolution of the perturbation we have monitored the evolution of the displacements u_i and of the velocities v_i of the beads versus the bead number i as a function of time. A snapshot of the solutions at a given time is shown in Fig. 2 and Fig. 3. The bead displacements are characterized by a front wave followed by inclined plateaus. The plateaus consist of an almost smooth curve with jumps. It is worth noting how, in the plot of the displacements, intervals with positive slopes typically correspond to regions of detached particles while the negative slopes correspond to particles in contact with each other. The snapshot for the velocities exhibits a structure of peaks with decreasing amplitude. These peaks correspond to waves propagating with monotonically decreasing velocities. Each wave is, at its turn, composed by several particles which are all in contact

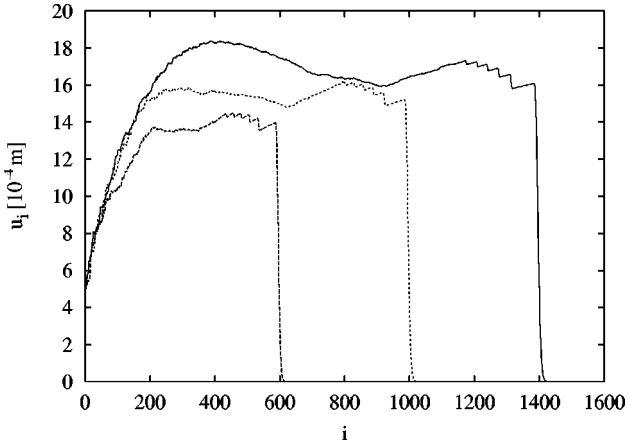

FIG. 2. Displacements of the beads at propagation times equal to 6×10^{-3} s, 10^{-2} s, and 1.4×10^{-2} s.

with each other and moving in the same forward direction. In between the peaks particles are not in contact and propagate in the backward direction with decreasing velocities. In Fig. 3 we also see the appearance of noise. This is a real numerical noise which is reduced but never disappears when we decrease the time step resolution. In fact, decreasing the resolution by one order of magnitude allows us to observe another peak and so on and so forth. In the ideal case of infinite resolution one would be able to observe an infinite series of peaks behind the front. As we shall see later, this fact has no consequences on our conclusions since we will discuss the region where no noise occurs and results can be extrapolated to the noisy region. Coming back to the analysis of Fig. 3 we can say that periodically the front loses energy when its last particle is detached, i.e., loses contact. This is the only way in which the energy stored in the front wave can decrease. In this way behind the front one has a chain of particles moving backward with decreasing velocity. These particles can eventually contribute to the formation of peaks whose nature is different from that of the front. We will come back to this point later when we will discuss the actual mechanism for the front formation.

It can be easily shown that the front wave propagates nearly at the sound velocity. In order to do that we calculate analytically the speed of sound in a medium of the same density as our beads and we compare the results with the

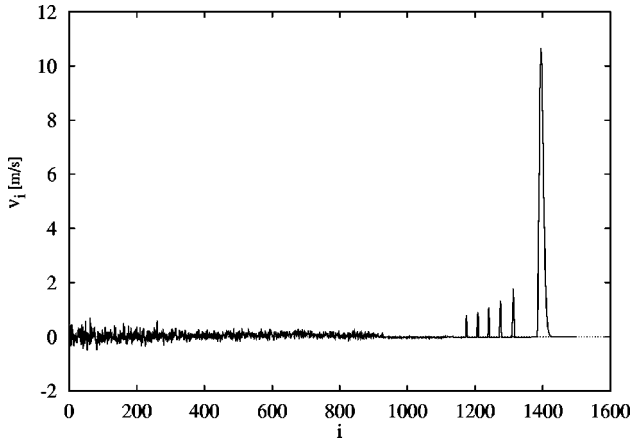

FIG. 3. Velocities of the beads after 1.4×10^{-2} s.

speed observed numerically for several values of the elastic constant k: 10^8 N m^{-1},10^7 N m^{-1}, and 10^6 N m^{-1}.

The calculation of the speed of sound is made as follows: if we consider the beads as springs of spring constant k and length $2R$ we get a dispersion relation that is

$$\omega = 2\sqrt{\frac{k}{m}}|\sin qR|, \tag{8}$$

where q is the wave vector. The speed of sound being defined by $c_s = \lim_{q\to 0}\omega/q$, we get

$$c_s = 2R\sqrt{\frac{k}{m}}. \tag{9}$$

Replacing all the parameters with their numerical values we have $c_s = 3170.47$ m s^{-1} when $k = 10^8$ N m^{-1}, $c_s = 1002.59$ m s^{-1} when $k = 10^7$ N m^{-1}, and $c_s = 317.05$ m s^{-1} when $k = 10^6$ N m^{-1}. These speeds are systematically slightly greater than the ones computed numerically which gave us 3160 m s^{-1},1000 m s^{-1}, and 316 m s^{-1}, respectively. These numerical values have been obtained by counting the number of beads separating the positions of the maxima of velocity in the front at two different times. We cannot thus pretend an exact agreement with theoretical values.

In order to have a better understanding of our results we compare our system with the harmonic chain consisting in a series of springs with spring constant k. We integrated the harmonic chain keeping the same initial conditions. After some algebra we get the chain eigenfrequencies:

$$\omega_l^2 = 4\frac{k}{m}\cos^2\frac{l\pi}{2N-1}, \quad 1 \leqslant l \leqslant N-1. \tag{10}$$

We then obtain for the displacements:

$$u_n(t) = \delta_0 + (-1)^n \sum_{l=1}^{N-1} C_l \sin(2nl\pi/2N-1)\cos\omega_l t,$$

$$1 \leqslant n \leqslant N-1$$

$$u_0(t) = \delta_0, \tag{11}$$

where the C_l are constants depending on the initial condition.

This relation is shown in Fig. 4 where we recognize the well-known oscillations after the front due to the discretization as already discussed by Gibbs and being now what we call the ''Gibbs phenomenon.'' We also plotted in Fig. 4 what happens when one tries to go continuously from the harmonic case to the no-tension case by decreasing the spring constant of the springs when they are under traction and keeping them equal to k under compression. Each curve corresponds to a different value of the ratio of the spring constant under traction over k. We clearly observe a continuous transition from the harmonic regime to the no-tension one as we decrease the ratio of the spring constants.

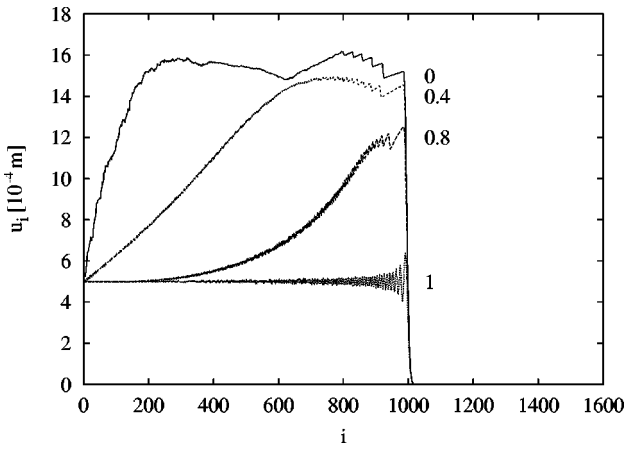

FIG. 4. Curves of displacements for different values for the ratio of the elasticity constants. The ratio goes from one (harmonic chain) to zero (nonlinear chain). The propagation time is 10^{-2} s.

IV. WAVE FORMATION

In the preceding section we have made some observations about the displacement and velocity profiles for a fixed time of propagation. Let us now consider the time evolution in order to understand how the peaks are created and how they propagate.

A. Scaling of the front shape

We define the amplitude of the front wave as the maximum velocity of the beads belonging to it. The curve representing this amplitude as a function of time is shown in Fig. 5. One can see that the amplitude decreases and oscillates. These oscillations are due to the discretization, i.e., to the fact that the bead having the maximum velocity keeps it during a finite time corresponding in Fig. 5 to the width of the oscillation. Initially the fastest bead has a low velocity that increases towards a maximum with time. Then this value decreases to a value lower than the initial value. This behavior continues with the right neighbor of the previous bead which then has the new maximum speed and keeps it during

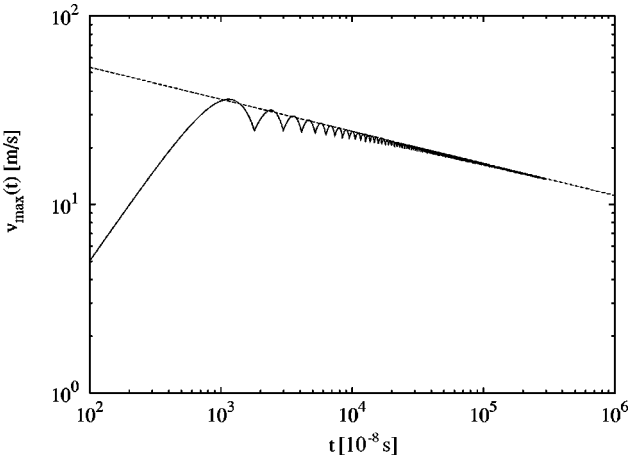

FIG. 5. Double-logarithmic plot of the amplitude of the front wave versus time. After a fast increase it decreases and oscillates. The dashed line corresponds to the function $f(x) \propto x^{-\alpha}$ which fits the envelope of the maxima of the amplitude curve.

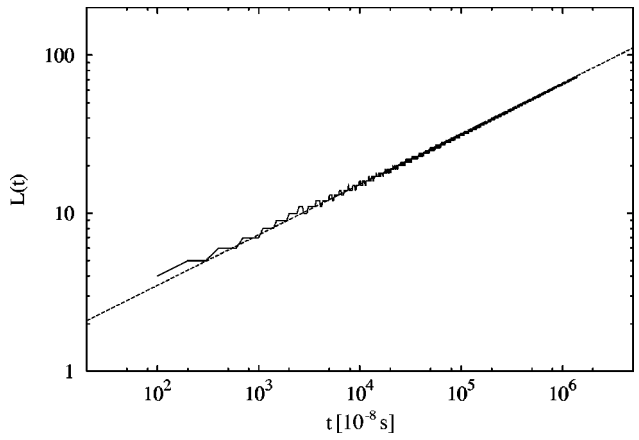

FIG. 6. Double-logarithmic plot of the width of the front wave versus time. The dashed line corresponds to the function $f(x) \propto x^{\beta}$ showing an increase of the width with a power law.

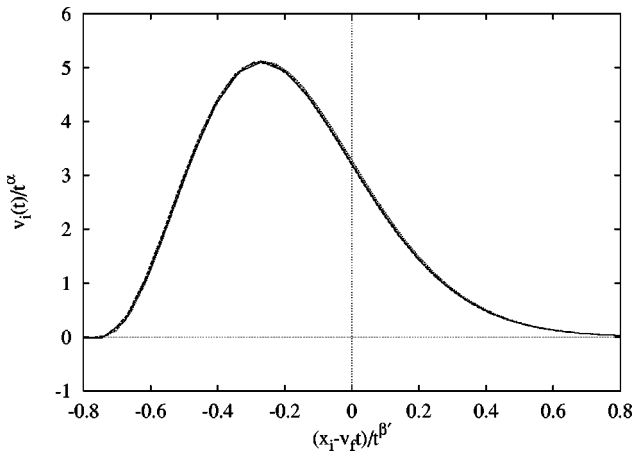

FIG. 7. Collapse of the front wave shape to a single curve verifying the scaling law for the bead velocities in the front wave. We show four curves corresponding to $t = 0.3 \times 10^{-2}$ s, 0.6×10^{-2} s, 0.9×10^{-2} s, 1.2×10^{-2} s. $\alpha = 0.17$, $\beta' = \frac{1}{3}$, and $v_f = 1001.5$ m s^{-1}.

a finite time with the same evolution as before. On a log-log scale we find that the envelope of the maxima is well fitted by a power law $A(t) \propto t^{-\alpha}$ with $\alpha \simeq 0.17$, consistent with a $t^{-1/6}$ behavior. This value of the exponent seems to be universal since it is robust when changing the value of the elasticity constant k in the range 10^6–10^8 and δ_0 in the range 0.3–0.7 mm.

We also define the width of the front wave by counting the number of beads with velocities greater than zero belonging to the front. For this quantity we find a scaling law $L(t) \propto t^{\beta}$ with $\beta \simeq 0.32$ (see Fig. 6). In this case the behavior is consistent with $t^{1/3}$ and is very robust with the same universal character as for the scaling of $A(t)$. The exponents α and β agree with the calculation made by Hinch [11] using the conservation of kinetic energy of the front wave ($\alpha' = \frac{1}{6}, \beta' = \frac{1}{3}$).

The use of the two previous power laws enables us to find a scaling relation for the front. By plotting $v_i(t)/t^{-\alpha}$ versus $(x_i - v_f t)/t^{\beta'}$ where v_f is an adjustable parameter with the dimension of a speed, we found that the curves corresponding to different values of t collapse on a single one as shown in Fig. 7. The collapse happens for a value of $v_f = 1001.5$ m s^{-1} which is very close to the sound speed 1002.5 m s^{-1} ($k = 10^7$ N m^{-1}). It is worth noting that v_f is the speed measured at the center of mass of the front and not at its maximum. The best collapse is obtained for the values of $\alpha = 0.17$ and $\beta' = \frac{1}{3}$. The exponent β changed to β' in agreement with the theoretical results whereas α is not exactly equal to α' since its calculation is based on kinetic energy conservation. In the present case energy is dissipated from the front wave by the effect of detachment of particles which induce a correction to α'. We can therefore write the following scaling law for the elastic front:

$$\frac{v_i(t)}{t^{-\alpha}} = f\left(\frac{x_i - v_f t}{t^{\beta'}}\right), \tag{12}$$

where f is a scaling function that has also been calculated [11] and $v_f = 1001.5$ m s^{-1}.

This scaling relation allows us to describe the self-similarity of the front wave shape. Another interesting feature coming from the scaling relation is that the velocity of the front is defined at the center of mass of the beads belonging to it. The other points on the front shape move with different velocities. Each point behind the center of mass moves with a velocity smaller than the sound speed whereas the points on the part preceding the center move with a larger velocity. Thus the front wave is divided into a subsonic and a supersonic part. This kind of wave is very different from the solitonic ones discovered by Nesterenko [8], who found that the wave travels with a constant shape and a constant speed for all its points.

B. Emergence of the secondary peaks

Let us now focus our attention on the secondary peaks propagating behind the elastic front. The particles detached from the front move backwards and their energy does the same (the system is globally conservative). This energy propagating backwards is then transferred from particle to particle until it reaches the left boundary where it is reflected and starts to propagate forward. This is the beginning of the propagation of a peak. The process then continues by means of detachments of particles from this peak, contributing in this way to the formation of new peaks.

In order to analyze in detail the evolution of the peaks we looked at the spatiotemporal structure of the contacts of the first 100 beads of the chain. This can be seen in Fig. 8: a gray dot means that there is a contact between two beads whereas a white dot means that they are not in contact. The computation of the contact distribution of the beads is done every 10^{-5} s up to a propagation time of 2.5×10^{-3} s. At 10^{-5} s almost all the beads are under compression. Then this compression chain moves to the right, leaving empty spaces between the first beads of the chain. This corresponds to the formation of the front wave. As the compression chain travels (the large gray triangle in the right lower corner of the plot) one can observe gray dots appearing at the beginning of the chain. This means that a new compression wave is being created. This wave is much thinner than the front wave and is represented on the plot by an almost straight curve with a slope slightly above the slope of the front, showing that this

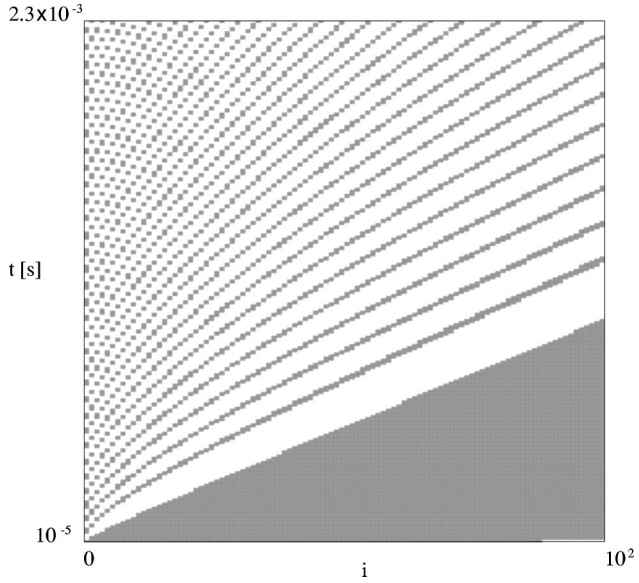

FIG. 8. Spatiotemporal evolution of bead contacts. The first 100 contact points of the chain are on the horizontal axis and time is on the vertical axis. The distribution of contacts is computed every 10^{-5} s. Here we started at 10^{-5} s till 2.5×10^{-3} s. A white square means that there is no contact between two beads whereas a gray one means that the beads are in contact.

first peak travels slower than the front. It can be seen that the other peaks are also formed at the begining of the chain, all making an almost straight gray line with a slowly increasing slope, which means a decreasing speed. It is easy to understand that the existence of these peaks is due to reflections on the first bead, which remains fixed, playing the role of a reflecting wall. Hence without noise there should be more than five peaks in Fig. 3: all the peaks behind these five have been destroyed by a numerical noise and one should see a succession of peaks with decreasing amplitude until the beginning of the chain. One more important point emerging from the spatiotemporal pattern is that beads which do not belong to a peak are not under compression and are thus in a ballistic regime, as one can see from the white spaces separating the peaks in Fig. 8.

V. CONCLUSION

We have studied the response of a chain of beads to a small displacement when no static force is applied to its ends. We observe a propagation of waves that is very different from the solitons which can be seen in a Hertzian chain.

The nonlinearity of the problem lies in the contact law used: a step function which indicates that there is no force when two beads are not in contact.

By keeping the left end of the chain fixed we observed an interesting bouncing phenomenon. In addition to the elastic front, secondary peaks of decreasing amplitude are generated at the left end of the chain. These peaks correspond to several beads in compression traveling in the forward direction whereas the beads in between the peaks travel in the backward direction without touching each other. We have found an interesting scaling law for the velocity of the beads belonging to the elastic front. This law, which has also been derived analytically by Hinch [11], seems to be universal since it does not depend on the parameters of the problem.

Starting from these results it would be interesting to look at a chain submitted to other types of perturbations. Besides, it is important to look at different networks (two or three dimensional) in order to understand the effect of the network structure on wave propagation.

ACKNOWLEDGMENTS

We recently became aware that Hinch [11] studied a very similar problem, getting very similar results. We thank him for having shown us his analytical results. We are also grateful to S. Roux for many interesting discussions. V.L. has been supported by Contract No. CEE ERBFMBICT 961220.

[1] H. M. Jaeger, S. R. Nagel, and R. P. Behringer, Rev. Mod. Phys. **68**, 1259 (1996).
[2] C. Liu, Phys. Rev. B **50**, 782 (1994).
[3] C. Liu and S. R. Nagel, Phys. Rev. Lett. **68**, 2301 (1992).
[4] C. Liu and S. R. Nagel, Phys. Rev. B **48**, 15 646 (1993).
[5] S. Feng and D. Sornette, Phys. Lett. A **184**, 127 (1993).
[6] S. Melin, Phys. Rev. E **49**, 2353 (1994).
[7] J. D. Goddard, Proc. R. Soc. London, Ser. A **430**, 105 (1990).
[8] V. F. Nesterenko, Prikl. Mekh. Tekh. Fiz. **5**, 136 (1983) [J. Appl. Mech. Tech. Phys. **24**, 567 (1983)].
[9] A. N. Lazaridi and V. F. Nesterenko, Prikl. Mekh. Tekh. Fiz. **3**, 115 (1985) [J. Appl. Mech. Tech. Phys. **26**, 405 (1985)].
[10] C. Coste, E. Falcon, and S. Fauve, Phys. Rev. E **56**, 6104 (1997).
[11] J. Hinch (unpublished).
[12] M. K. Alves and B. K. Alves, Eur. J. Mech. A/Solids **16**, 103 (1997).